Fiber Breakage and Fiber Pull-Out of Fiber-Reinforced Ceramic-Matrix Composites

François Hild, Alain Burr, Frederick A. Leckie

Fiber breakage and fiber pull-out of fiber-reinforced ceramic-matrix composites

F. HILD*, **, A. BURR*, ** and F. A. LECKIE*

ABSTRACT. – Fiber breakage and fiber pull-out induce loss of stiffness, anelastic strains, hysteresis loops, and crack closure. Ultimate strength properties of fiber-reinforced composites are derived and compared with results related to localization. These features are analyzed in the framework of Continuum Mechanics through the introduction of internal variables. Three models which are progressively more faithful to the micromechanical analysis are studied. They provide guidance on the choice of the relevant internal variables to model the mechanical behavior of unidirectional fiber-reinforced composites.

1. Introduction

Ceramic-Matrix Composites (CMC's) are potential candidates to meet the new goals of high performance structures, especially when the elements are subjected to high mechanical and thermal load histories [URI, 1994]. Their low density combined with high strength and good performance at high temperature are appealing features in the design of new generation jet engines.

This paper is part of an effort to derive constitutive equations which describe the behavior of CMC's within the context of Continuum Damage Mechanics (CDM). The approach makes use of the micromechanical analyses of the degradation mechanisms occurring in CMC's. The degradation mechanisms include matrix cracking and fiber breakage both of which are accompanied by slip at the fiber/matrix interface. Matrix cracking which first forms at quite low stresses continues to grow with increasing stress until saturation is reached when the application of increased stress does not increase the crack density. The saturation is usually the consequence of the shear induced by the interface between fibers and matrix [Aveston *et al.*, 1971]. Starting from a material which is assumed free from any initial macro defect, the mechanical behavior is predicted by using Continuum Damage Mechanics. The results presented herein are valid when the steady matrix cracking stress [Budiansky *et al.*, 1986] is less than the ultimate strength of a fiber-reinforced composite [Budiansky, 1993]. When this hypothesis is satisfied, the key

* Department of Mechanical and Environmental Engineering, University of California, Santa Barbara CA 93106-5070, U.S.A.

** Also at Laboratoire de Mécanique et Technologie, E.N.S. de Cachan/C.N.R.S./Université Paris-VI, 61, avenue du Président-Wilson, F-94235 Cachan Cedex, France.

mechanism leading to final failure is fiber breakage. For this reason no attempt is made to model the growth of matrix craking and saturation conditions are assumed. The fiber breakage mechanism is accompanied by distributed fiber pull-out when broken fibers pulling out of the matrix introduce shear stresses along the interface. This mechanism distinguishes the behavior of fiber-reinforced CMC's from that of the classical dry fiber bundle [Coleman, 1958].

The ultimate tensile strength at localization of strain is calculated for unidirectional composites and a micromechanics analysis of unloading-reloading sequences is developed, when hysteresis loops are formed. The micromechanics models are used to evaluate three different constitutive laws which are progressively more faithful to the micromechanical analysis. It is shown in practice that it is not always necessary to model all the details revealed by micromechanics. Previous studies by Hild *et al.* [Hild *et al.*, 1994 *b*] indicate that by identifying the relevant internal variables of a Continuum Damage Mechanics description the studies of unidirectional composites can be extended readily to the 2-*D* constitutive laws applicable to multidirectional lay ups under complex loading conditions.

2. Expression of the ultimate tensile strength

A unit cell of length L_R (*Fig.* 1 *a*) is considered where the matrix cracks are saturated with spacing L_m. The length L_R is the *recovery* length and refers to twice the longest fiber that can be pulled out and cause a reduction in the load carrying capacity. Away from a fiber break, as in the case of matrix cracking, the fiber stress builds up through the stress transfer across the sliding fiber-matrix interface. If the interfacial shear stress τ is assumed to be constant, the recovery length is related to the maximum stress in the fiber by [Curtin, 1991]

$$L_R = \frac{RT}{\tau} \tag{1}$$

where the reference stress T is the fiber stress in the plane of the matrix crack, R is the fiber radius. Generally, $L_m \ll L_R$ and the stress field in the intact fibers [Cox, 1952; Kelly, 1973] for $0 \leq x \leq \frac{L_m}{2}$ is (*Fig.* 1 *b*)

$$\sigma_F(T, x) = T - \frac{2\tau}{R} x \tag{2}$$

If the fibers exhibit a statistical variation of strength that obeys a two-parameter Weibull law [Weibull, 1939], then the probability that a fiber would break anywhere within the recovery length L_R at or below a reference stress T is given by

$$P_F(T) = 1 - \exp\left\{-\frac{2}{L_0}\int_0^{L_R/2}\left\{\frac{\sigma_F(T, x)}{S_0}\right\}^m dx\right\} \tag{3}$$

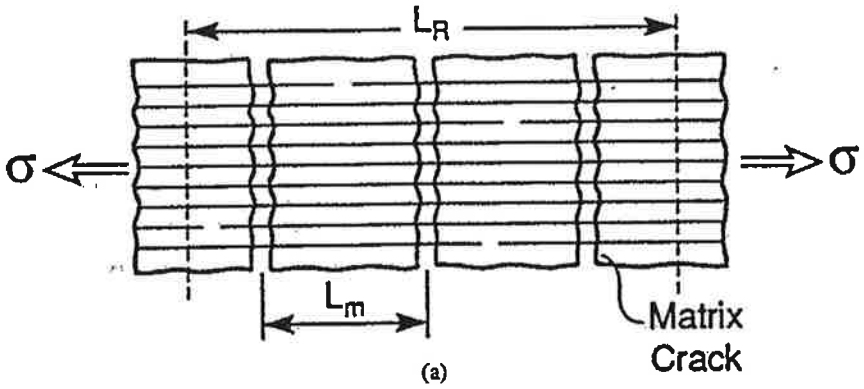

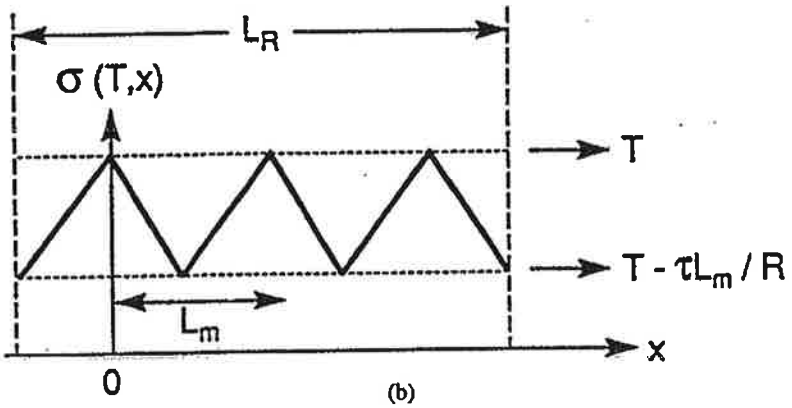

Fig. 1 *a*. – Depiction of the recovery length L_R when the density of matrix cracks (characterized by L_m) reaches saturation.

Fig. 1 *b*. – Fiber stress field $\sigma_F(T, x)$ along a length L_R for a reference stress T when the fibers are intact.

where m is the shape parameter, S_0 is the stress scale parameter, and L_0 a reference length. Eqn. (3) can be simplified when $L_m/L_R \ll 1$ to become

$$P_F(T) = 1 - \exp\left\{-\left(\frac{T}{S_c}\right)^{m+1}\right\} \tag{4}$$

where S_c denotes the *characteristic strength* [Henstenburg & Phoenix, 1989]

$$S_c^{m+1} = \frac{L_0\, S_0^m\, \tau}{R} \tag{5}$$

The relevant length to consider is the recovery length instead of the total length of the composite [Cao & Thouless, 1990]. The cumulative failure probability is thus *independent* of the total length of the composite, provided the total length of the composite is greater than the recovery length [Hild *et al.*, 1994 *a*]. The average stress $\bar{\sigma}$ applied to the composite is related to the reference stress T by

$$\bar{\sigma} = f\,T\,\{1 - P_F(T)\} + \bar{\sigma}_{FP}(T) = \bar{\sigma}_{FB}(T) + \bar{\sigma}_{FP}(T) \tag{6}$$

where f is the fiber volume fraction, $\bar{\sigma}_{FB}(T)$ denotes that component of the stress provided by *unbroken fibers*, and $\bar{\sigma}_{FP}(T)$ denotes that component of the stress provided

by *failed fibers* as they pull out from the matrix. For global load sharing [Curtin, 1993], the pull-out stress is given is given by

$$\bar{\sigma}_{FP}(T) = f\, P_F(T)\, \bar{\sigma}_b(T) \tag{7}$$

where $\bar{\sigma}_b(T)$ denotes the average stress at a plane of matrix crack $x = 0$ when a fiber breaks at location $x = t$, and at the reference stress level T. When the load is assumed to be homogeneous over the entire composite length, the average pull-out stress $\bar{\sigma}_b(T)$ reduces to $T/2$, and the external stress takes the form

$$\bar{\sigma} = f\, T\, \{1 - P_F(T)\} + f\, \frac{T}{2}\, P_F(T) \tag{8}$$

In Figure 2, the contributions of the two mechanisms are plotted for $m = 4$. The pull-out stress is a strictly increasing function, whereas the stress in the unbroken fibers reaches a maximum value. Because of the decrease of the stress $\bar{\sigma}_{FB}$, an ultimate stress exists. This decrease leads to a loss of uniqueness of the stress-strain relationship. Indeed, elastic unloading of the unbroken fibers may arise in one part of the composite and further fiber breakage in another part. Consequently localization appears and Eqn. (8) after that point corresponds to the homogeneous solution, which usually cannot be reached [Hild & Burr, 1994]. The applied stress level corresponding to the onset of localization will be referred to as localization tensile strength, and will be denoted by $\bar{\sigma}_{LTS}$. In the framework of CDM, the initiation of a macrocrack is described as a localization of the deformations [Billardon & Doghri, 1989], which corresponds to the onset of a surface across which the velocity gradient is discontinuous. Physically, it corresponds to localized pull-out,

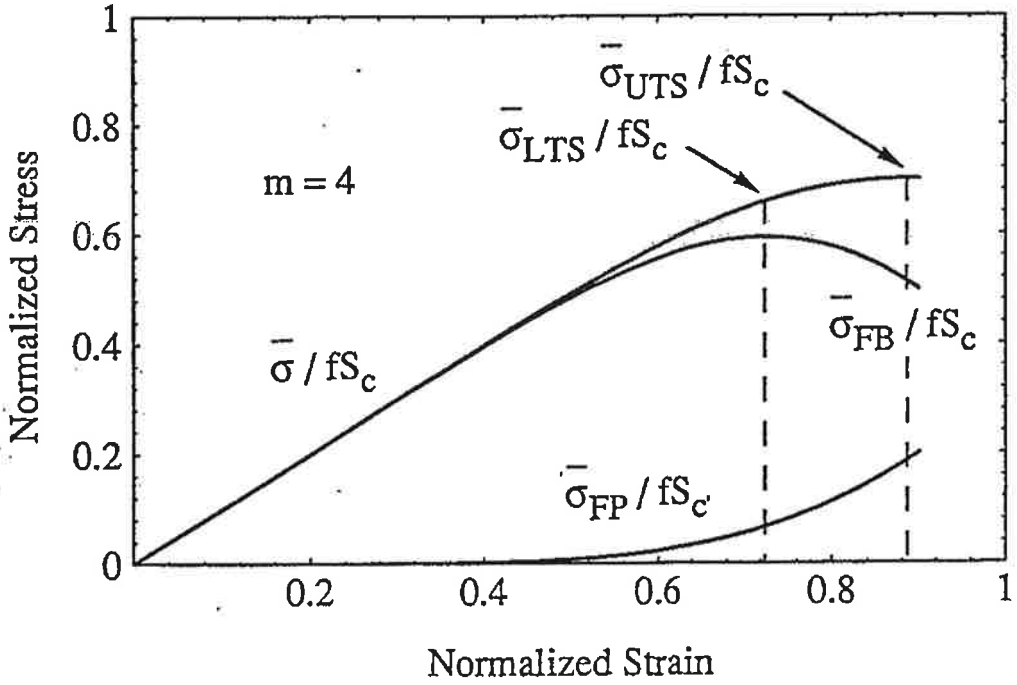

Fig. 2. – Normalized stresses, $\bar{\sigma}/f\,S_c$, $\bar{\sigma}_{FB}/f\,S_c$, $\bar{\sigma}_{FP}/f\,S_c$ versus normalized strain, $\bar{\varepsilon}\,E_F/S_c$.

whereby one macrocrack develops and pull-out continues to evolve in the vicinity of that macrocrack only. This phenomenon leads to a different behavior as compared to the homogeneous solution for which damage is still evolving in a diffusive manner. Under small deformations assumption, localization is mainly driven by the damage mechanism that causes strain softening [Lemaitre, 1992]. The localization tensile strength of the composite is defined by the condition

$$d\bar{\sigma}_{FB}/d\bar{\varepsilon} = 0 \tag{9}$$

or

$$d\bar{\sigma}_{FB}/dT = 0 \tag{10}$$

because the reference stress T is proportional to the average strain on the composite according to the relation,

$$\bar{\varepsilon} = \frac{2}{L_m}\int_0^{L_m/2} \frac{\sigma_F(T, x)}{E_F}\, dx \cong \frac{T}{E_F} \tag{11}$$

where E_F denotes the Young's modulus of the *unbroken* fibers. Consequently, the localization tensile strength becomes

$$\bar{\sigma}_{LTS} = \frac{f S_c}{2}\left(\frac{1}{m+1}\right)^{1/(m+1)}\left\{1 + \exp\left(-\frac{1}{m+1}\right)\right\} \tag{12}$$

The ultimate tensile strength of the composite is defined by the condition

$$d\bar{\sigma}/d\bar{\varepsilon} = 0 \tag{13}$$

This equation cannot be solved analytically. A first order solution of the ultimate tensile strength, $\bar{\sigma}_{UTS}$, is predicted to be [C, 1991]

$$\bar{\sigma}_{UTS} = f S_c\left(\frac{2}{m+2}\right)^{1/(m+1)}\frac{m+1}{m+2} \tag{14}$$

3. Unloading-reloading sequence

The consequences of unloading followed by a reloading sequence are now investigated. Reversed motion of fibers relative to the matrix has been studied by numerous authors [Marshall & Oliver, 1987; McMeeking & Evans, 1990]. After reaching a maximum value characterized by T_M (less than the localization level), and by the maximum friction length L_{FM}, which is equal to half the maximum recovery length, L_{RM}, the load is reversed (*Fig.* 3). The maximum friction length is therefore related to the maximum reference stress T_M by

$$L_{FM}(T_M) = \frac{RT_M}{2\tau} \tag{15}$$

Upon unloading, in the range, $0 \leq |z| \leq L_{FU}$, there is a reversal of both the relative sliding direction and the frictional shear stress (*Fig.* 3). For $L_{FU} \leq |z| \leq L_{FM}$, the shear stress there remains unchanged from that prevailing during the loading process. The actual load level is characterized by the reference stress $T = T_M - \Delta T_U$, and the unloading friction length L_{FU} is related to ΔT_U by

$$L_{FU} = \frac{R\,\Delta T_U}{4\tau} = L_{FM}\left(\frac{\Delta T_U}{2}\right) \tag{16}$$

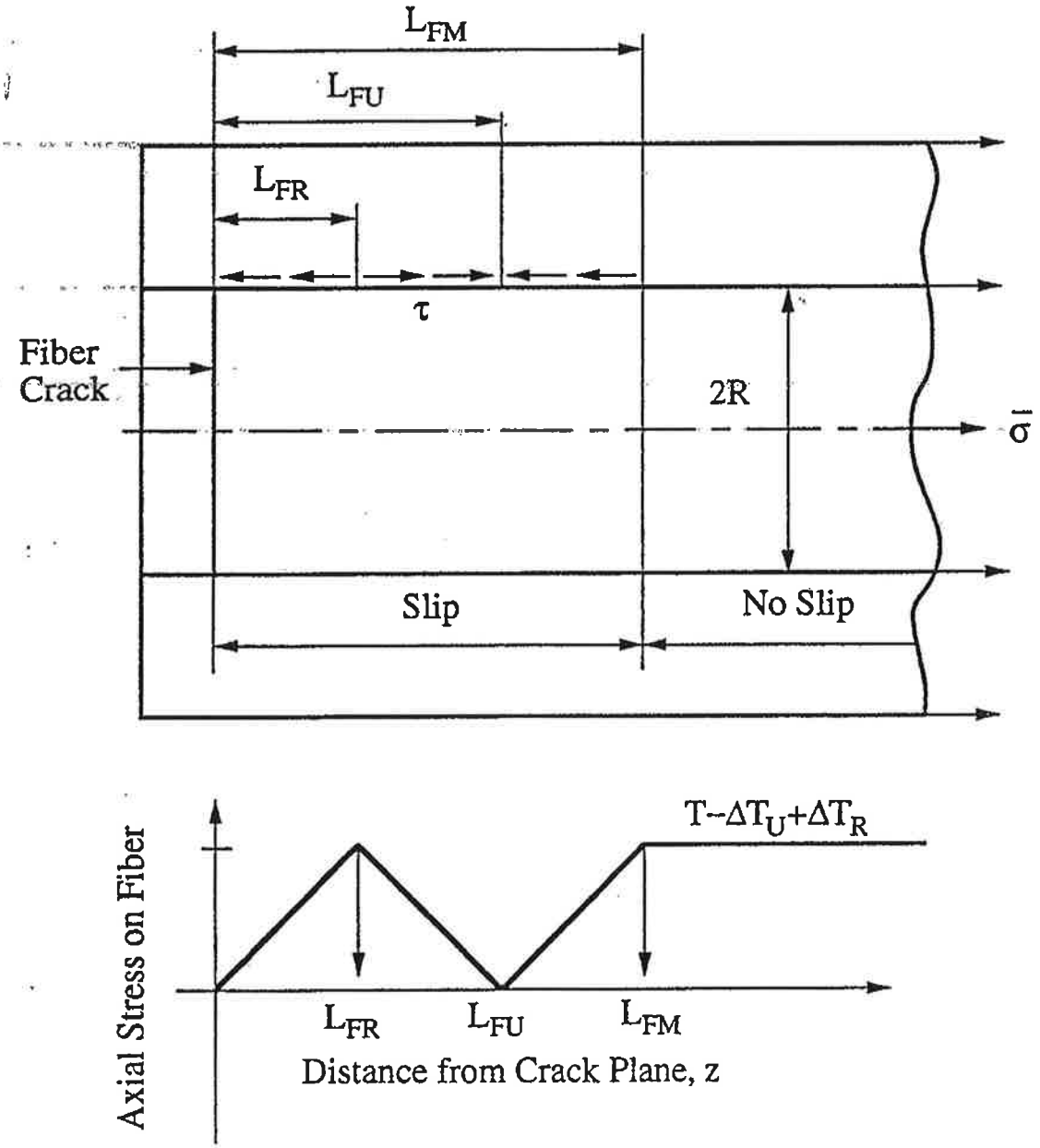

Fig. 3. – Depiction of the friction length, L_F, upon loading, the unloading friction length, L_{FU}, the reloading friction length, L_{FR}, and the corresponding axial stress on a broken fiber embedded in matrix.

Then, the external stress takes the form

$$\frac{\bar{\sigma}}{f} = (T_M - \Delta T_U) - \frac{P_F(T_M)}{4}\,\frac{2T_M^2 - \Delta T_U^2}{T_M} \tag{17}$$

Because of fiber pull-out, anelastic strains exist after complete unloading ($\bar{\sigma} = 0$). When $\bar{\sigma} = 0$, the expression of the unloading amplitude $\Delta T_U = T_M$ is

$$T_m = \frac{2T_M - \sqrt{2}T_M\sqrt{1 + (1 - P_F(T_M))^2}}{P_F(T_M)} \tag{18}$$

for which, the corresponding anelastic strains are given by

$$\bar{\varepsilon}_{an} = \frac{T_M - T_m}{E_F} \tag{19}$$

The anelastic strains depend upon the maximum load level, and the percentage of broken fibers, $P_F(T_M)$, within the recovery length L_{RM}. In Figure 4 the anelastic strains are plotted as a function of the maximum load level T_M. Their evolution which is a non-linear function of the maximum applied strains indicates that the anelastic strains are an order of magnitude smaller than the maximum total applied strain.

If unloading continues below T_m, there is closure of the fiber cracks when $\Delta T_U = T_c$ given by

$$T_c = \sqrt{2}T_M \tag{20}$$

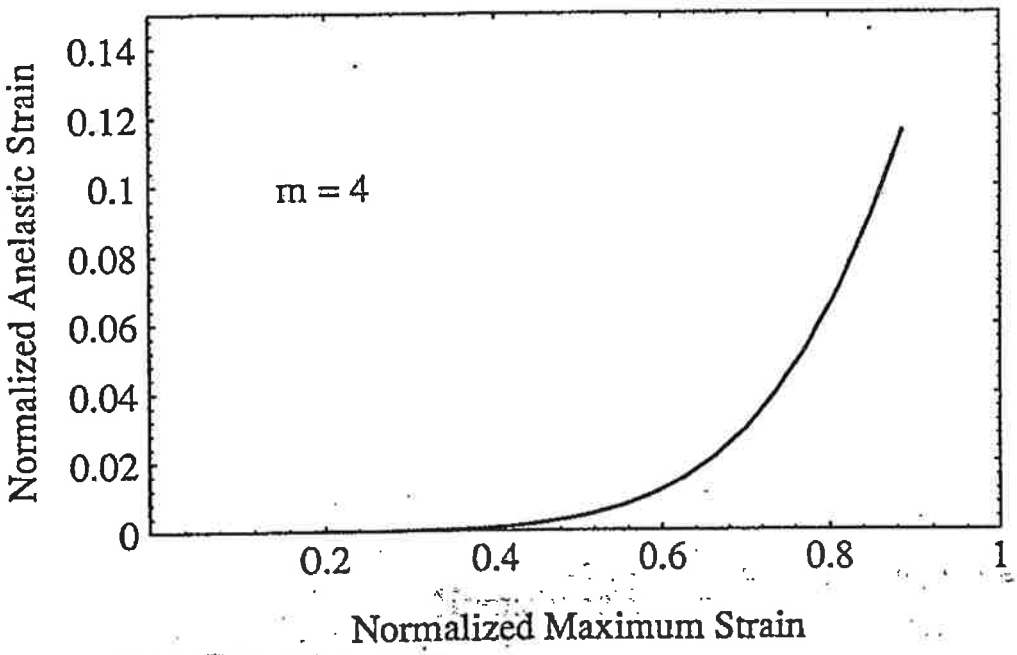

Fig. 4. – Normalized anelastic strain, $\bar{\varepsilon}_{an}\,(\bar{\sigma} = 0)\,E_F/S_c$ as a function of normalized strain, $\bar{\varepsilon}\,E_F/S_c$.

The unloading and the closure phenomenon can be described in terms of the difference in displacement between a broken face and an adjacent unbroken fiber, measured by δ (*Fig.* 5). The displacement δ is referred to as crack opening displacement. When δ is positive, there is pull-out, when δ is equal to zero, there is no pull-out since closure takes over. During the unloading sequence, the expression of the crack opening is given by

$$\delta(T_M, \Delta T_U) = \frac{R(2T_M^2 - \Delta T_U^2)}{8\tau E_F} \tag{21}$$

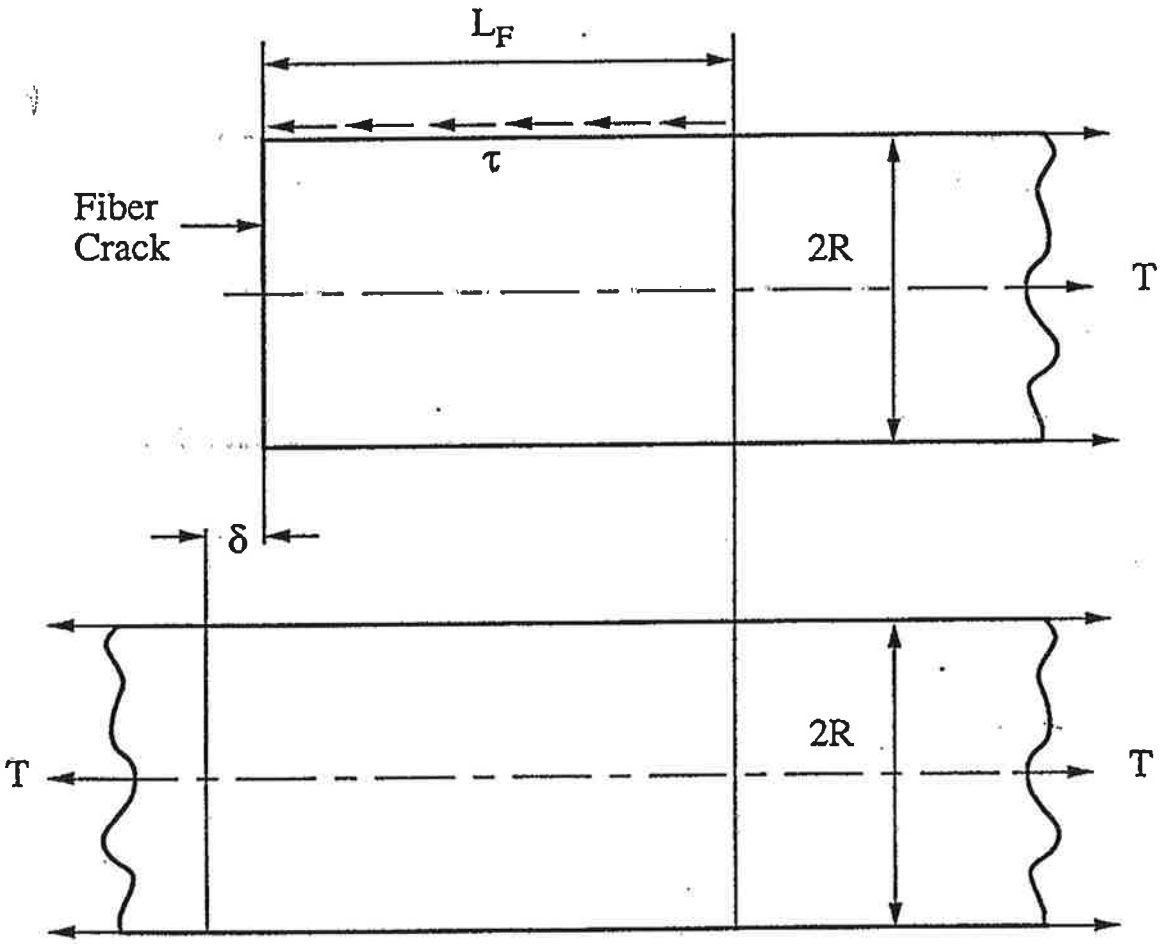

Fig. 5. – Depiction of the opening displacement δ.

After reaching a minimum value characterized by the amplitude T_m of the reference stress, and by the reverse friction length L_{Fm}, the load is reversed again (*Fig.* 3). It then leads to a reloading process. Upon reloading, characterized by $T = T_M - T_m + \Delta T_R$, sliding is confined to $0 \leq |z| \leq L_{FR}$,

$$L_{FR} = \frac{R\,\Delta T_R}{4\tau} \tag{22}$$

Then, the external stress takes the form

$$\frac{\bar{\sigma}}{f} = (T_M - T_m + \Delta T_R) - \frac{P_F(T_M)}{4}\,\frac{2T_M^2 - T_m^2 + \Delta T_R^2}{T_M} \tag{23}$$

In Figure 6 a loading-unloading-reloading sequence is plotted. The non-linear effects are the consequence of fiber breakage leading to a reduced Young's modulus, and fiber pull-out inducing friction and anelastic strains. If no wear mechanisms is involved, this first cycle corresponds to the steady state cycle. One way of characterizing the hysteresis loops is to measure their maximum width, $\delta\bar{\varepsilon}$. In Figure 7 the maximum hysteresis loop width is plotted as a function of maximum strain. Again, the evolution is non-linear wrt. the maximum applied strains.

Lastly it is possible to calculate the evolution of the crack opening during the reloading sequence to give

$$\delta(T_M, \Delta T_m, \Delta T_R) = \frac{R(2T_M^2 - T_m^2 + \Delta T_R^2)}{8\tau E_F} \tag{24}$$

During a loading-unloading-reloading sequence, the pull-out stress, $\bar{\sigma}_{FP}(T_M, T_m, \Delta T_R)$, is related to the crack opening displacement measured during the sequence, $\delta(T_M, T_m, \Delta T_R)$, by

$$\bar{\sigma}_{FP}(T_M, T_m, \Delta T_R) = \left(\bar{\varepsilon} - \frac{\delta(T_M, T_m, \Delta T_R)}{L_{FM}}\right) f E_F P_F(T_M) \tag{25}$$

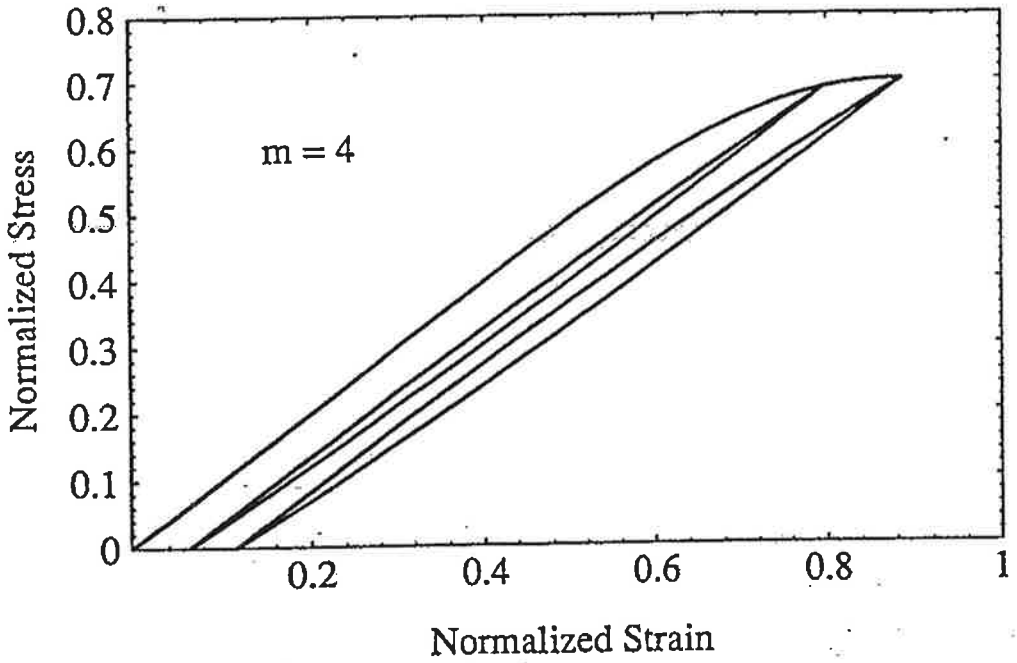

Fig. 6. – Normalized stress, $\bar{\sigma}/f\,S_c$, versus normalized strain, $\bar{\varepsilon}\,E_F/S_c$, during a loading-unloading-reloading sequence.

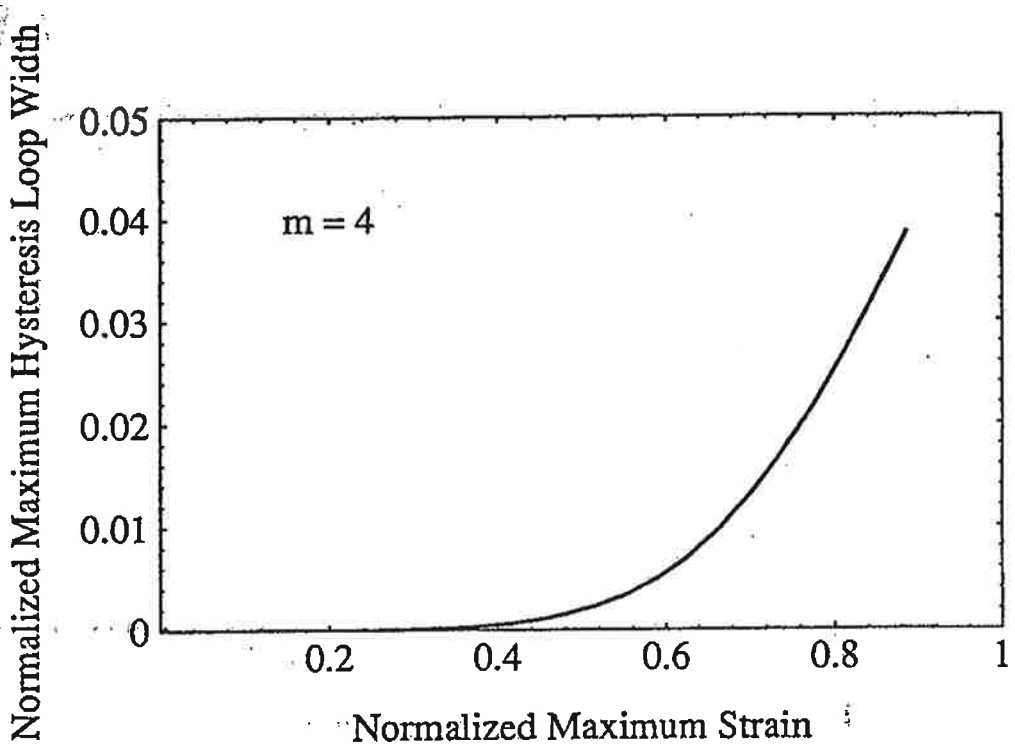

Fig. 7. – Normalized maximum hysteresis loop width, $\delta\bar{\varepsilon}\,E_F/S_c$ as a function of maximum normalized strain, $\bar{\varepsilon}\,E_F/S_c$.

This micromechanical analysis enabled us to study loading and unloading sequences when fiber breakage and fiber pull-out are considered. In the next Section, the previous results will be modeled in the framework of Continuum Mechanics.

4. Continuum mechanics modeling

The micromechanical analysis shows that fiber breakage induces a reduction in stiffness, anelastic strains due to slipping at the matrix/fiber interface of broken fibers, and hysteresis loops due to reverse slipping upon unloading-reloading. In the following development, three different approaches are considered within the framework of Continuum Mechanics which model some or all of the features of the micromechanical model, depending on the degree of accuracy desired.

Within the framework of the thermodynamics of irreversible process [Bataille & Kestin, 1979; Germain *et al.*, 1983], the first step is to determine the state variables which describe the internal mechanisms which define the behavior of a material. The second step is to determine the state potential in terms of the state variables and the third step is to write the evolution laws of the internal variables. For the sake of simplicity, a one dimensional description will follow.

4.1. First model – fiber breakage

In this simplest model, only fiber breakage is considered and the effects of slip are neglected. This model predicts a reduction in stiffness as fibers break, but is unable to

model anelastic strains and hysteresis loops (*Fig.* 8). Because fiber breakage is a softening mechanism localization is possible (Section 2). In this case, the microscopic description of damage is the percentage of broken fibers in a cell of length $2L_F = L_R$ and is identical to the change of macroscopic stiffness. The damage variable D is therefore equal to $P_F(\bar{\varepsilon})$, and the stress strain relationship can be written as follows

$$\bar{\sigma} = f E_F (1 - D) \bar{\varepsilon} \tag{26}$$

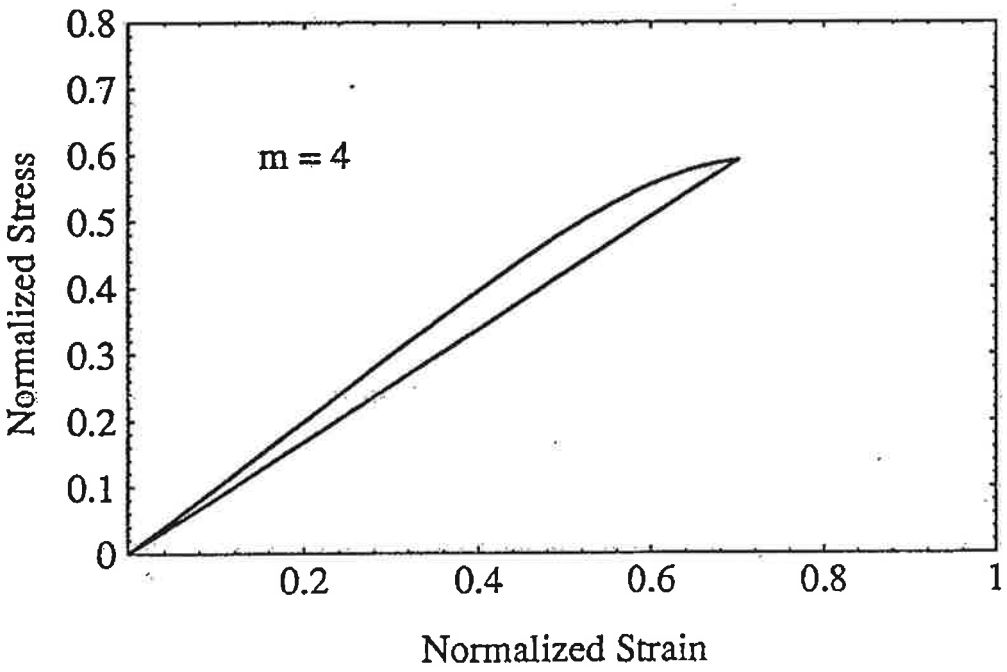

Fig. 8. – Normalized stress, $\bar{\sigma}/f S_c$, versus normalized strain, $\bar{\varepsilon} E_F/S_c$, during a loading-unloading-reloading sequence for model No. 1.

The damage variable D evolves as the maximum value of $\bar{\varepsilon}$ increases during a loading sequence $0 \leq \xi \leq t$. On the other hand, when $\bar{\varepsilon}$ decreases, the percentage of broken fibers remains constant. Furthermore, only positive strains (or stresses) lead to fiber breakage

$$D = P_F \left(\operatorname*{Max}_{0 \leq \xi \leq t} \langle \bar{\varepsilon}(\xi) \rangle \right) \tag{27}$$

where $\langle \cdot \rangle$ denotes the Macauley brackets. This latter condition can be rewritten as

$$\overset{\circ}{D} = \begin{cases} \dfrac{dP_F(\bar{\varepsilon})}{d\bar{\varepsilon}} \overset{\circ}{\bar{\varepsilon}} & \text{if } \dfrac{d}{dt} \operatorname*{Max}_{0 \leq \xi \leq t} \langle \bar{\varepsilon}(\xi) \rangle > 0 \\ 0 & \text{otherwise} \end{cases} \tag{28}$$

The above results can also be derived by using two potentials following the procedure described by Lemaitre and Chaboche [Lemaitre & Chaboche, 1985]. The first potential

is the Helmholtz free energy density, ψ. The second potential is the pseudo-potential of dissipation, F, which defines the growth rate of the state variables. Since no friction is involved when fiber break the elastic energy density is written as

$$\psi = \frac{f E_F}{2} (1 - D) \bar{\varepsilon}^2 \tag{29}$$

The expression of the external applied stress is given by the partial derivation of ψ wrt. $\bar{\varepsilon}$ which gives the same result as Eqn. (26). The thermodynamic force associated with the damage variable D is defined as the partial derivative of ψ wrt. the damage variable D. If Y denotes the associated thermodynamic force then

$$Y = -\frac{\partial \psi}{\partial D} = \frac{f E_F}{2} \bar{\varepsilon}^2 \tag{30}$$

In the framework of Continuum Damage Mechanics, Y is refered to as the damage energy release rate density [Chaboche, 1978]. The evolution law satisfies the second principle of thermodynamics since the dissipation Φ is positive

$$\Phi = Y \, \overset{\circ}{D} \geq 0 \tag{31}$$

Since Y is positive definite, $\overset{\circ}{D}$ is positive, *i.e.* damage always increases and therefore accounts only for deterioration of materials (here fiber breakage). Let us now postulate that the kinetic laws are derived from a pseudo-potential of dissipation, F. The function F is a scalar continuous function of the dual variables (here Y), the state variables having the possibility to act as parameters (here D). If the function F is a convex function, and if the kinetic laws are derived by means of a positive scalar multiplier, $\overset{\circ}{\lambda}$, then the second principle of thermodynamics is always satisfied. Within the so-called normality rule of generalized standard materials, the kinetic law is selected to be

$$\overset{\circ}{D} = \begin{cases} \overset{\circ}{\lambda} \dfrac{\partial F}{\partial Y} & \text{if} \quad F = 0 \quad \text{and} \quad \overset{\circ}{F} = 0 \\ 0 & \text{if} \quad F < 0 \quad \text{or} \quad \overset{\circ}{F} < 0 \end{cases} \tag{32}$$

with

$$F = 1 - \exp\left\{ -\left(\frac{Y}{Y_c} \right)^{(m+1)/2} \right\} - D \qquad \text{and} \qquad Y_c = \frac{1}{2} \frac{f S_c^2}{E_F}$$

The value of the multiplier $\overset{\circ}{\lambda}$ is determined by using the consistency condition $\overset{\circ}{F} = 0$. The expression of the multiplier is here given by

$$\overset{\circ}{\lambda} = \overset{\circ}{Y} \tag{33}$$

It is worth noting that Eqn. (32) which is written in terms of Continuum Damage Mechanics is completely equivalent to Eqns. (27) and (28).

4.2. Second model - fiber breakage and pull-out

This second model introduces the contribution of fiber breakage and fiber pull-out, but neglects hysteresis loops (*Fig.* 9). The features that are modeled are the reduction in stiffness due to fiber breakage and the anelastic strains due to fiber pull-out. It is assumed that the unloading process is linear, and is characterized by the damage $\bar{D}$. Therefore, the expression of the state potential ψ is written as [L & C, 1985]

$$\psi = \frac{f E_F}{2} (1 - \bar{D}) (\bar{\varepsilon} - \bar{\varepsilon}_{an})^2 \tag{34}$$

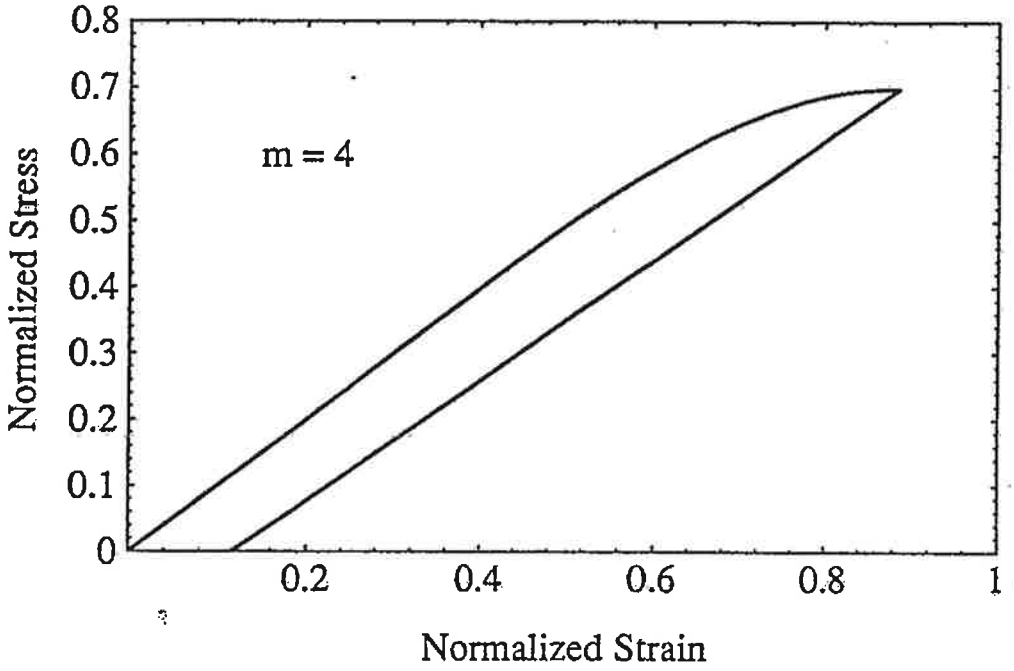

Fig. 9. – Normalized stress, $\bar{\sigma}/f S_c$, versus normalized strain, $\bar{\varepsilon} E_F/S_c$, during a loading-unloading-reloading sequence for model No. 2.

The state laws are obtained by partial differentiation of ψ wrt. the state variables

$$\begin{cases} \bar{\sigma} = \dfrac{\partial \psi}{\partial \bar{\varepsilon}} = f E_F (1 - \bar{D}) (\bar{\varepsilon} - \bar{\varepsilon}_{an}) \\ \bar{\sigma} = -\dfrac{\partial \psi}{\partial \bar{\varepsilon}_{an}} \\ \bar{Y} = -\dfrac{\partial \psi}{\partial \bar{D}} = \dfrac{f E_F}{2} (\bar{\varepsilon} - \bar{\varepsilon}_{an})^2 \end{cases} \tag{35}$$

Using Eqns. (18) and (19) of the micromechanical model, the anelastic strains are related to the maximum strain level, $\bar{\varepsilon}_M = \underset{0 \le \xi \le t}{\text{Max}} \langle \bar{\varepsilon}(\xi) \rangle$, and to the cumulative failure probability $P_F(\bar{\varepsilon}_M)$ by

$$\bar{\varepsilon}_{an} = \bar{\varepsilon}_M \left(1 - \frac{2 - \sqrt{2}\sqrt{1 + (1 - P_F(\bar{\varepsilon}_M))^2}}{P_F(\bar{\varepsilon}_M)} \right) \tag{36}$$

The damage variable $\bar{D}$ corresponding to the unloading modulus and is related to the cumulative failure probability by

$$\bar{D} = 1 - \frac{P_F(\bar{\varepsilon}_M)\left(1 - \frac{P_F(\bar{\varepsilon}_M)}{2}\right)}{2 - \sqrt{2}\sqrt{1 + (1 - P_F(\bar{\varepsilon}_M))^2}} \tag{37}$$

Eqn. (37) gives the relationship between the microscopic damage variable, $D = P_F(\bar{\varepsilon}_M)$, defined in the previous sub-Section and the macroscopic damage variable, $\bar{D}$. The evolution laws of the anelastic strains and the macroscopic damage variables derived in the micromechanical model are defined in Eqns. (36) and (37).

The dissipation Φ is now

$$\Phi = \bar{\sigma}\ \overset{\circ}{\bar{\varepsilon}}_{an} + \bar{Y}\ \overset{\circ}{\bar{D}} \geq 0 \tag{38}$$

and is positive. It is not easy to derive a simple expression for F and this has not been attempted. The evolution laws are written in terms of the maximum strains reached during the loading history. These laws are therefore directly integrated laws.

In this sub-Section, the approach was from a macroscopic point of view. Here we can see some apparent differences between the quantities at a micro level and macro level. These quantities are of course related but their significance is different, depending on the scale at which the observations are made. For example, the macroscopic damage variable $\bar{D}$ is related to the microscopic damage variable D by Eqn. (37). Furthermore, as shown in Section 2, localization predicted by this model (leading to the ultimate tensile stress) arises later than localization at a micro scale (localization tensile strength). This is due to the fact the softening mechanism at a micro scale is counter-balanced by the strengthening mechanism due to fiber pull-out up to the ultimate point. This law corresponds to the homogeneous solution after localization at the micro level.

4.3. Third model – micro mechanics based model

The model now discussed takes account of all three features induced by fiber breakage and fiber pull-out, viz. the reduction in stiffness due to fiber breakage, the anelastic strains due to fiber pull-out, and the hysteresis loops. The model is based on the micro mechanical study described previously (*Fig.* 6). The details of the unloading and reloading process are complex and to avoid this difficulty it is useful to introduce the crack opening displacement δ, which characterizes the material state related to the reverse friction. The crack opening displacement δ is also useful in determining the conditions when closure occurs. To characterize the state of the composite, four quantities are required. These are the overall strain $\bar{\varepsilon}$, the friction length L_F, the percentage of broken fibers, P_F, within the recovery length $L_R = 2L_F$, and the crack opening displacement, δ. To derive the free energy density associated to a loading sequence, we consider two different elastic steps to reach the same state. The first step consists in moving the unbroken fibers wrt.

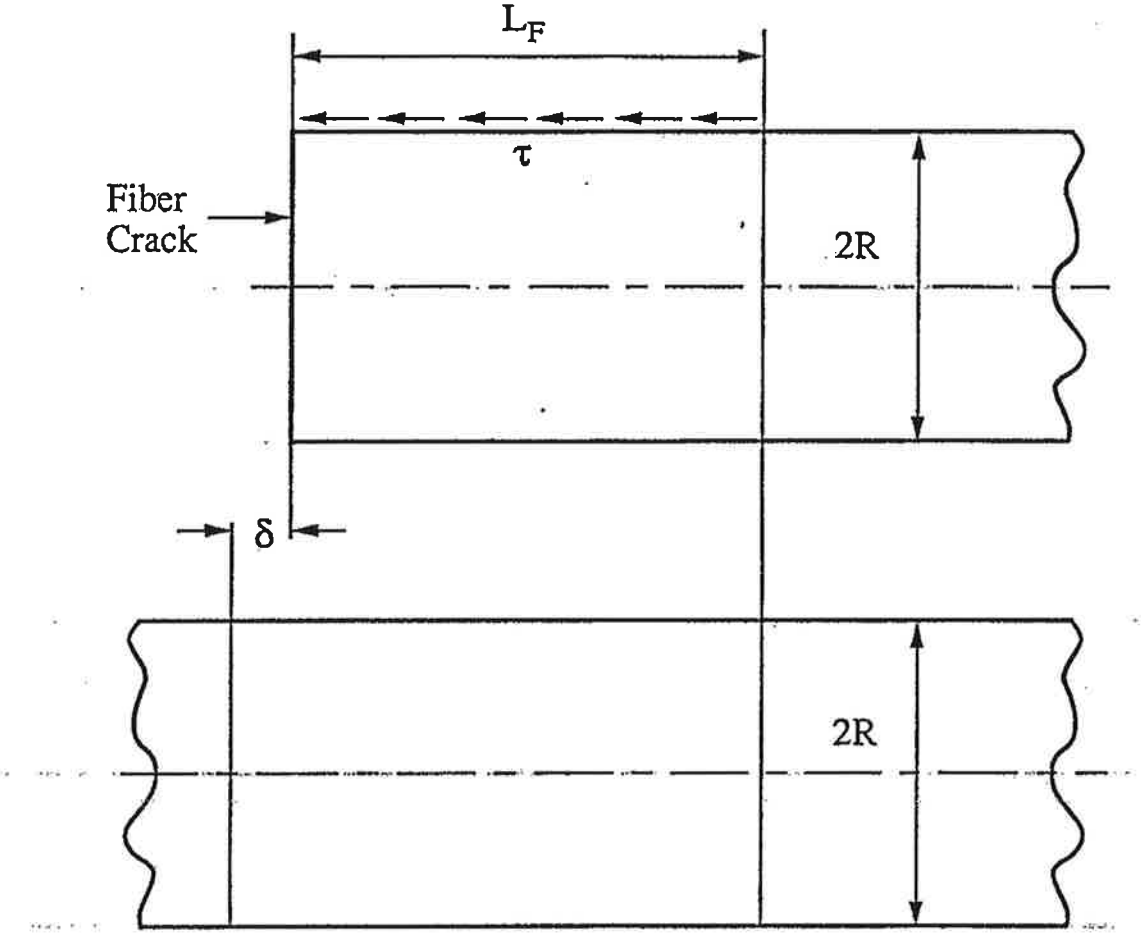

Fig. 10. – Motion of the unbroken fibers wrt. the broken fibers with no external load by an amount δ over a length L_F.

the broken fibers with no external load by an amount δ over a length L_F (*Fig.* 10). The elastic energy density associated with this process is given by

$$\psi^s = \frac{f E_F}{2} \left(\frac{\delta}{L_F} \right)^2 P_F \frac{4 - 3 P_F}{3} \tag{39}$$

The opening displacement δ induces an overall anelastic strain α

$$\alpha = \frac{\delta}{L_F} P_F \tag{40}$$

It is worth noting that $\bar{\varepsilon}_{an} = \alpha$ when $\bar{\sigma} = 0$. The second step, during which no friction occurs, consists in adding an elastic loading from the previous state. It involves an additional elastic energy density given by

$$\psi^e = \frac{f E_F}{2} (\bar{\varepsilon} - \alpha)^2 \tag{41}$$

The total free energy density is then sum of the two energies. A more convenient expression for the free energy density is obtained by using state variables in a modified

form. The state variables are the total strain, $\bar{\varepsilon}$, the damage variable modeling the percentage of broken fibers, $D = P_F$, and the anelastic strains α due to the crack opening displacement δ modeling the fiber pull-out mechanism. The opening strain α is similar to a kinematic hardening variable, and the associated force corresponds to the back-stress induced by the slipping mechanism. The free energy density ψ can then be written in terms of the new internal variables

$$\psi = \frac{f E_F}{2} (\bar{\varepsilon} - \alpha)^2 + \frac{f E_F}{2} \frac{4 - 3D}{3D} \alpha^2 \tag{42}$$

The thermodynamic forces associated with the new state variables are respectively given by

$$\begin{cases} \bar{\sigma} = \dfrac{\partial \psi}{\partial \bar{\varepsilon}} = f E_F (\bar{\varepsilon} - \alpha) & (43.1) \\ Y = -\dfrac{\partial \psi}{\partial D} = \dfrac{2 f E_F}{3} \left(\dfrac{\alpha}{D}\right)^2 & (43.2) \\ X = \dfrac{\partial \psi}{\partial \alpha} = f E_F \left(\dfrac{4\alpha}{3D} - \bar{\varepsilon}\right) & (43.3) \end{cases}$$

The evolution laws of the damage variable is directly given by the evolution of the cumulative failure probability P_F:

$$D = P_F \left(\underset{0 \le \xi \le t}{\text{Max}} \langle \bar{\varepsilon}(\xi) \rangle \right) \tag{44}$$

The evolution law of the internal variable α uses the results derived during the loading-unloading-reloading sequence. Upon loading, the evolution of α is given by

$$\alpha = \frac{1}{2} \underset{0 \le \xi \le t}{\text{Max}} \langle \bar{\varepsilon}(\xi) \rangle \, P_F \left(\underset{0 \le \xi \le t}{\text{Max}} \langle \bar{\varepsilon}(\xi) \rangle \right) \tag{45.1}$$

The variation of α, $\Delta\alpha = \alpha - \alpha_0$, wrt. minimum or maximum value, α_0 (corresponding to a maximum loading or minimum unloading level characterized by $\bar{\varepsilon}_0$) is related to the strain variation, $\Delta\bar{\varepsilon} = \bar{\varepsilon} - \bar{\varepsilon}_0$, by

$$\Delta\alpha = \frac{1}{4} \frac{(\Delta\bar{\varepsilon})^2}{\underset{0 \le \xi \le t}{\text{Max}} \langle \bar{\varepsilon}(\xi) \rangle} \text{Sign}(\Delta\bar{\varepsilon}) \, P_F \left(\underset{0 \le \xi \le t}{\text{Max}} \langle \bar{\varepsilon}(\xi) \rangle \right) \tag{45.2}$$

Instead of the complicated pattern of friction and reverse friction descrided in the micro mechanical analysis, a single macroscopic variable is introduced. This is the opening strain which corresponds to the crack opening displacement. It is worth remembering that this last model captures the essential features related to fiber breakage and fiber pull-out and that it is able to predict the localization tensile strength. Furthermore,

the crack closure condition can be obtained by computing that α vanishes, *i.e.* when $\Delta\bar{\varepsilon} = \sqrt{2} \underset{0\leq\xi\leq t}{\text{Max}} \langle \bar{\varepsilon}(\xi) \rangle$. This last result shows that α cannot be negative. Moreover, the free energy density catches this crack closure phenomenon, and does not correspond to a partition in positive/negative strains or positive/negative stresses as is usually assumed [L, 1992]. The dissipation Φ

$$\Phi = -X \overset{\circ}{\alpha} + Y \overset{\circ}{D} \geq 0 \tag{46}$$

is positive during a loading sequence. The condition given in Eqn. (46) is strong [Onat & Leckie, 1988] and is not satisfied during part of the unloading or reloaging sequence. On the other hand, during a complete unloading-reloading sequence, the dissipated energy over one cycle is given by

$$\Delta\Phi = \frac{f E_F}{2} \left\{ \frac{P_F(\bar{\varepsilon}_M)}{6} \frac{(\bar{\varepsilon}_M - \bar{\varepsilon}_m)^3}{\bar{\varepsilon}_M} \right\} \tag{47}$$

which is a positive quantity, in accordance with the second principle of thermodynamics.

5. Conclusions

In this paper models have been developed which describe the mechanisms of fiber breakage and fiber pull-out. Upon loading, fiber breakage induces a softening behavior whereas fiber pull-out induces strengthening. Because of fiber breakage, loss of uniqueness and localization appear before the peak of the macroscopic stress/strain response in tension.

A micromechanical model is derived which describes the loading and unloading-reloading sequences. These sequences induce slip and reverse slip. Because of fiber pull-out, permanent strains appear upon complete unloading. Moreover, hysteresis loops are observed upon unloading and reloading. These hysteresis loops characterize the amount of energy that is dissipated during one unloading-reloading cycle. A convenient means of characterizing the sequences is to introduce the crack opening displacement between broken and unbroken fibers.

In the framework of Continuum Mechanics, three models have been studied. The first model was concerned with fiber breakage modeled by an internal variable called damage and corresponding to the percentage of broken fibers within a relevant length, the recovery length. This model is able to predict loss of stiffness and localization, but not anelastic strains nor hysteresis loops. The second model was based on the loss of stiffness and the anelastic strains. It was able to model the loading portion, anelastic strains, but not localization on a microscopic level nor hysteresis loops. The third model considered two internal variables, which are the damage at a microscopic level, and an opening strain proportional to the crack opening displacement divided by the friction. This model was able to capture all the details of the microscopic study with only two internal variables.

This last model will constitute the basis of a constitutive law applied to Ceramic-Matrix Composites subject to complex loading conditions. In particular the knowledge of the free energy density, the internal variables and their associated forces are crucial. These laws have to be generalized under more complex loading conditions, as well as composite architectures. In the case of more complex architectures, the interaction between fibers in different directions has to be assessed, especially in the case of woven configurations.

Acknowledgments

This work was supported by the Defense Advanced Research Project Agency through the University Research Initiative under Office of Naval Research Contract No. N-00014-92-J-1808.

REFERENCES

AVESTON J., COOPER G. A., KELLY A., 1971, Single and Multiple Fracture, in *Conference Proceedings of the National Physical Laboratory: Properties of Fiber Composites*, IPC Sciences and Technologie Press, Surrey, England, 15-26.

BATAILLE J., KESTIN J., 1979, Irreversible Processes and Physical Interpretations of Rational Thermodynamics, *J Non Equil. Thermodynamics*, 4, 229-258.

BILLARDON R., DOGHRI I., 1989, Prévision de l'amorçage d'une macro-fissure par la localisation de l'endommagement, *C. R. Acad. Sci., Paris*, 308, Series II, 347-352.

BUDIANSKY B., 1993, Tensile Strength of Aligned-Fiber Composites, *University Research Initiative*, Winter Study Group, University of California, Santa Barbara.

BUDIANSKY B., HUTCHINSON J. W., EVANS A. G., 1986, Matrix Fracture in Fiber-Reinforced Ceramics, *J. Mech. Phys. Solids*, 34, 167-189.

CAO H. C., THOULESS M. D., 1990, Tensile Tests of Ceramic-Matrix Composites: Theory and Experiments, *J. Am. Ceram. Soc.*, 73, [7], 2091-2094.

CHABOCHE J.-L., 1978, Description thermodynamique et phénoménologique de la viscoplasticité cyclique avec endommagement, *Thèse de doctorat de l'État*, Université Paris-VI.

COLEMAN B. D., 1958, On the Strength of Classical Fibers and Fibers Bundles, *J. Mech. Phys. Solids*, 7, 60-70.

COX H. L., 1952, The elasticity and the strength of paper and other fibrous Materials, *Br. J. Appl. Phys.*, 3, 72-79.

CURTIN W. A., 1991, Theory of Mechanical Properties of Ceramic Matrix Composites, *J. Am. Ceram. Soc.*, 74, [11], 2837-2845.

CURTIN W. A., 1993, The "Tough" to Brittle Transition in Brittle Matrix Composites, *J. Mech. Phys. Solids*, 41, [2], 217-245.

GERMAIN P., NGUYEN Q. S., SUQUET P., 1983, Continuum Thermodynamics, *J. Appl. Mech.*, 50, 1010-1020.

HENSTENBURG R. B., PHOENIX, 1989, Interfacial Shear Strength Using Single-Filament-Composite Test. Part II: A Probability Model and Monte Carlo Simulations, *Polym. Comp.*, 10, [5], 389-406.

HILD F., BURR A., 1994, Localization and Ultimate Strength of Fiber-Reinforced Ceramic-Matrix Composites, *Mech. Res. Comm.*, 21, [4], 297-302.

HILD F., DOMERGUE J.-M., EVANS A. G., LECKIE F. A., 1994 *a*, Tensile and Flexural Ultimate Strength of Fiber Reinforced Ceramic-Matrix Composites, *Int. J. Solids Struct.*, 31, [7], 1035-1045.

HILD F., LARSSON P.-L., LECKIE F. A., 1994 *b*, Localization due to Damage in two Direction Fiber-Reinforced Composites, *J. Appl. Mech.*, accepted.

KELLY A., 1973, Chapter 5, in *Strong Solids*, Oxford University Press, 2nd edn.

LEMAITRE J., 1992, *A Course on Damage Mechanics*, Springer-Verlag, Berlin.

LEMAITRE J., CHABOCHE J.-L., 1985, *Mécanique des matériaux solides*, Dunod, Paris. English translation: *Mechanics of Solid Materials*, Cambridge University Press, Cambridge, 1990.

MARSHALL D. B., OLIVIER W. C., 1987, Measurement of Interfacial Mechanical Properties in Fiber-Reinforced Ceramic Composites, *J. Am. Ceram. Soc.*, 70, 542-548.

McMeeking R. M., Evans A. G., 1990, Matrix Fatigue Cracking in Fiber Composites, *Mech. Mat.*, **9**, 217-227.
Onat E. T., Leckie F. A., 1988, Representation of Mechanical Behavior in the Presence of Changing Internal Structure, *J. Appl. Mech.*, **55**, 1-10.
URI, 1994, Winter Study Group, University of California, Santa Barbara (USA).
Weibull W., 1939, A Statistical Theory of the Strength of Materials, 151, *Royal Swed. Inst. For Eng. Res.*